INTERNATIONAL JOURNAL FOR NUMERICAL METHODS IN ENGINEERING
Int. J. Numer. Meth. Engng. **45**, 473–490 (1999)

THIN-WALLED CLOSED BOX BEAM ELEMENT FOR STATIC AND DYNAMIC ANALYSIS

YOON YOUNG KIM*,† AND JIN HONG KIM‡

Department of Mechanical Design, Seoul National University, Kwanak-Gu, Shinlim-Dong, San 56-1, Seoul 151-742, Korea

SUMMARY

A new displacement-based finite element is developed for thin-walled box beams. Unlike the existing elements, dealing with either static problems alone or dynamic problems only with the additional consideration of warping, the present element is useful for both static and dynamic analyses with the consideration of coupled deformation of torsion, warping and distortion. We propose to use a statically admissible in-plane displacement field for the element stiffness matrix and a kinematically compatible displacement field for the mass matrix so that the present element is useful for a wide range of beam width-to-height ratios. The axial variation of cross-sectional deformation measures is approximated by C^0 continuous interpolation functions. Numerical examples are considered to confirm the validity of the present element. Copyright © 1999 John Wiley & Sons, Ltd.

KEY WORDS: thin-walled closed box beam; finite element; warping; distortion

INTRODUCTION

Thin-walled beams have been widely used in many engineering applications because of the high stiffness-to-mass ratio. In particular, thin-walled beams with closed cross-sections are very important structural elements when high torsional and bending rigidities are required. For instance, most load-carrying members in automobiles and airplanes are made of thin-walled closed beams.

There are a number of good finite beam elements which are based on the Timoshenko beam theory [1], but they lack possibility to consider some aspects of thin-walled closed beams. These elements typically have six degrees of freedom at each node consisting of three translations and three rotations, but warping and distortion cannot be handled by these elements. There are elements which can incorporate warping deformation in open beams. However, there appears no available beam element that includes distortion as well as warping deformations of thin-walled closed beams.

Vlasov [2] provides a comprehensive theoretical treatment of thin-walled structures including closed beams. Kříštek [3] solves the problem of non-uniform torsion in tapered box beams and considers the effect of a force deforming the cross section. Finite beam element formulation for the static analysis of thin-walled box beams with insufficient transverse stiffening is presented by

* Correspondence to: Yoon Young Kim, Department of Mechanical Design and Production Engineering, Seoul National University, Kwanak-Gu, Shinlim-Dong, San 56-1, Seoul 151-742, Korea. E-mail: yykim@plaza.snu.ac.kr
† Associate Professor
‡ Graduate Student

CCC 0029–5981/99/160473–18$17.50

Received 26 January 1998
Revised 3 September 1998

Boswell and Zhang [4], who develop C^1 continuous element. Boswell and Zhang [5] later propose the distortional function characterized by a single parameter in order to investigate distortional effects. They also present experimental results on the same subject [6]. Zhang and Lyons [7, 8] develop a multi-cell box finite beam element for the analysis of curved bridges, and Boswell and Li [9] discuss warping functions due to the torsion and distortion. Razaqpur and Li [10, 11] study multi-cell box beams with the consideration of warping functions for shear lag effects and distortional deformation. They also extend their theory to curved thin-walled box beams [12]. Mikkola and Paavola [13] suggest the finite element method for elastic box beams. Paavola [14] presents a discrete finite element method in which the cross sections are assumed to consist of piecewise rectilinear cross sections of separate shells. Similarly, Prokic [15] constructs the warping function having the number of degrees of freedom equal to the number of the corner points of the beam cross section. Although all these methods are successful for static analysis, none of them appears to be suitable for dynamic as well as static analyses. Indeed, no direct extension of any of these methods to dynamic analysis has been reported.

For thin-walled beam dynamic analysis, Gere [16] has carried out the torsional vibration analysis of open section beams. Recently, Bishop *et al.* [17], Friberg [18], Zhang and Chen [19], Kou *et al.* [20], and Kim *et al.* [21, 22] perform the dynamic analysis of thin-walled beams, but only warping effects are considered in these analyses. Laudiero and Savoia [23] carry out vibration analysis based on trigonometric series.

Although some papers are focused on the dynamic analysis of thin-walled closed beams, no paper was found that carries out the finite element analysis of a thin-walled closed beam taking into account the complete coupling of torsion, warping and distortion deformations. It should be again pointed out that the existing finite element formulations for thin-walled closed box beams appear neither suitable nor efficient for the extension to dynamic analysis.

We remark here that the sectional distortion of thin-walled closed beams contributes considerably to lowering the natural frequency of torsion-dominant vibration modes. Therefore, both distortional and warping deformations must be included in order to predict the dynamic behavior of thin-walled beams correctly. Balch [24] and Balch and Steele [25] discuss in depth the significant local effects associated with warping and sectional distortion near the joints of thin-walled closed beams such as in H-frames. Kim *et al.* [26] address the significant effects of warping and distortion on the dynamic behavior of thin-walled box beam T-joints.

We start directly with the kinematic variables, describing torsional, warping and distortional deformations in a thin-walled closed box beam. Subsequently, the present finite element is suitable for both static and dynamic analyses and is perhaps the first finite element that takes distortional deformations into account for dynamic analysis. Furthermore, we propose to use different functions for in-plane distortional displacement fields for the construction of element stiffness and mass matrices. For the stiffness matrix, the in-plane displacement field obtained directly from Vlasov's theory is selected to satisfy the equilibrium condition, not the continuity condition. On the other hand, we select the in-plane displacement field satisfying the continuity, not equilibrium for the construction of the element mass matrix. This has been done since it is difficult to find the in-plane distortional displacement functions that satisfy both the equilibrium and compatibility conditions without introducing complications.

The axial variation of cross-sectional deformation measures is approximated with typical two-node elements with linearly varying C^0 continuous interpolation functions. Obviously, more elaborate approaches using the concepts of field-consistency, reduced integration, or mixed formulation may be used to improve numerical results. However, a simple C^0 displacement-based formulation

will be used as this paper aims at showing a possibility of developing a thin-walled closed-beam finite element that can be used for both static and dynamic analyses with the consideration of distortional deformations.

Although a thin-walled box beam has a simple geometry, the box beam may be adequate to show most of the complicated coupled deformations of torsion, warping and distortion. The advantage of working with this geometry is that bending and axial deformations uncouple with the deformations associated with twist, warping and distortion; the present finite element analysis can be focused only on the important characteristics of these deformations. Subsequently, only the deformations of twist, warping and distortion will be investigated in the present work. However, the analysis of this box beam will serve as a first step towards the analysis of more complicated, general thin-walled closed beams. To verify the validity of the present thin-walled closed box beam element, numerical examples are considered.

DISPLACEMENT FIELD AND GOVERNING EQUATIONS

We consider a thin-walled closed box beam shown in Figure 1. The beam width and height are denoted by b and h. The beam is assumed to be of uniform thickness t, and length L. In the analysis of this beam, the thickness is assumed to be much smaller than the other dimensions. Furthermore, the contour that is the middle surface of the plates that constitute the thin-walled beam is assumed to be in-extensional. For the complete discussion of all the assumptions, see [2].

In Figure 1, a right-handed curvilinear co-ordinate system (n,s,z) is used in addition to the Cartesian co-ordinate system (x, y, z). The tangential co-ordinate s is measured along the contour. The normal co-ordinate n directs outwards from the surface as indicated in the figure. Since the bending and axial deformations decouple with the coupled deformation of twist, warping and in-plane distortion in the box beam, we will consider only the finite element analysis for the displacement field associated with twist, warping and distortion. Bending and axial deformations can be easily analyzed by existing beam elements based on the Euler or Timoshenko beam theories.

It is convenient to describe the displacement of a point on the contour in terms of the normal $u_n(s,z)$, tangential $u_s(s,z)$ and axial $u_z(s,z)$ components as indicated in Figure 1. These displacements are often referred to as shell displacements since their dependence on the tangential co-ordinate s appears explicitly. If the beam deformation at given z is denoted by the amounts of axial rotation $\theta(z)$, warping $U(z)$ and distortion $\chi(z)$, the shell displacements may be written as

$$u_s(s,z) = \psi_s^{\theta}(s)\theta(z) + \psi_s^{U}(s)U(z) + \psi_s^{\chi}(s)\chi(z) \tag{1a}$$

$$u_n(s,z) = \psi_n^{\theta}(s)\theta(z) + \psi_n^{U}(s)U(z) + \psi_n^{\chi}(s)\chi(z) \tag{1b}$$

$$u_z(s,z) = \psi_z^{\theta}(s)\theta(z) + \psi_z^{U}(s)U(z) + \psi_z^{\chi}(s)\chi(z) \tag{1c}$$

where $\psi(s)$ denote the functions describing how the contour deforms in the n–s plane.

By considering only the rotation $\theta(z)$ of the beam cross-section about the positive z-axis, one can show that

$$\begin{aligned} \psi_s^{\theta}(s) &= r(s) \\ \psi_n^{\theta}(s) &= -\frac{l_{\text{side}}}{2} + s \\ \psi_z^{\theta}(s) &= 0 \end{aligned} \tag{2}$$

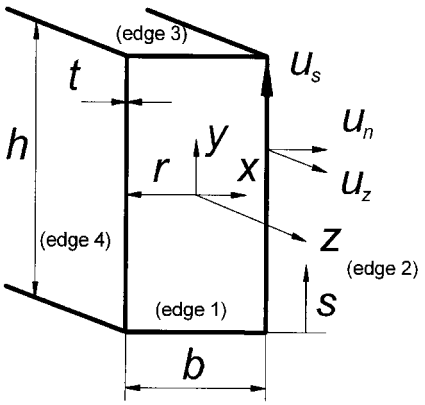

Figure 1. Displacements at an arbitrary point on the contour of a box beam (the edge wall thickness t is assumed to be uniform)

where $r(s)$ is the distance normal to the contour from the shear center of the cross section which is the same as the centroid, and l_{side} denotes the length of each edge of the beam in consideration. For the expressions in equation (2), the origin of the s co-ordinate is located at the starting point of each edge.

When warping deformation $U(z)$ is considered only, the shell displacements can be shown to be

$$\begin{aligned} \psi_s^U(s) &= 0 \\ \psi_n^U(s) &= 0 \\ \psi_z^U(s) &= x(s)y(s) \end{aligned} \tag{3}$$

Now considering in-plane distortional (or lozenging) deformation $\chi(z)$, the corresponding form of ψ can be found as [2]

$$\psi_s^\chi(s) = \left[\frac{\mathrm{d}x(s)}{\mathrm{d}s}y(s) + x(s)\frac{\mathrm{d}y(s)}{\mathrm{d}s}\right] \tag{4a}$$

$$\psi_n^\chi(s) = \left(-\frac{l_{\text{side}}}{2} + \frac{3}{l_{\text{side}}}s^2 - \frac{2}{l_{\text{side}}^2}s^3\right)(-1)^{i+1}\alpha, \quad i \text{ is edge number} \tag{4b}$$

$$\psi_z^\chi(s) = 0 \tag{4c}$$

with

$$\alpha = \begin{cases} \dfrac{2b}{b+h} & \text{for edges 1, 3} \\ \dfrac{2h}{b+h} & \text{for edges 2, 4} \end{cases} \tag{5}$$

Vlasov [2] determines the value of α in order to satisfy the moment equilibrium and maintain the right angle at each corner of the cross-sectional plane during the distortional deformation. However, the displacement field with the values of α given in equation (5) is not continuous at the corners of the cross section when the width is not the same as the height; α in equation (5) is so

selected as to satisfy mainly the static force equilibrium. However, in the dynamic analysis of the box beam, particularly in the calculation of the kinetic energy, the satisfaction of the displacement continuity may be more important than the satisfaction of the force equilibrium at the corners. Unfortunately, it is difficult to find the displacement field that satisfies both conditions by the form of equation (1). Subsequently, we propose to use a statically admissible displacement field in the construction of the element stiffness matrix and a kinematically compatible displacement field in the construction of the element mass matrix. As a result, the value of α in equation (5) given by Vlasov will be used for the construction of the stiffness matrix and the unit value of α that will guarantee the displacement continuity will be used for the construction of the mass matrix. For the case of α equal to 1, the function ψ_n^{χ} will be denoted by $\psi_n^{\chi^*}$ in the subsequent analysis.

The three-dimensional displacement field ($\tilde{u}_n$, $\tilde{u}_s$ and $\tilde{u}_z$) of thin-walled closed beams can be constructed from the shell displacements:

$$\begin{aligned}\tilde{u}_n(n,s,z) &\approx u_n(s,z)\\ &= \psi_n^{\theta}(s)\theta(z) + \psi_n^{\chi}(s)\chi(z) \qquad (6a)\\ \tilde{u}_s(n,s,z) &\approx u_s(s,z) + n\frac{\partial u_n(s,z)}{\partial s}\\ &\approx \psi_s^{\theta}(s)\theta(z) + \psi_s^{\chi}(s)\chi(z) + n\frac{\mathrm{d}\psi_n^{\chi}(s)}{\mathrm{d}s}\chi(z) \qquad (6b)\\ \tilde{u}_z(n,s,z) &\approx u_z(s,z)\\ &= \psi_z^{U}(s)U(z) \qquad (6c)\end{aligned}$$

The normals to the contour are assumed to remain straight and normal during deformation. The last term in equation (6b) may be neglected in expressing the kinetic energy, but this term should be considered in the calculation of strain.

Using the definition of strains and equation (6), the non-negligible three-dimensional strain components are

$$\begin{aligned}\varepsilon_{zz} &= \frac{\partial \tilde{u}_z}{\partial z} = \psi_z^{U}(s)\frac{\mathrm{d}U(z)}{\mathrm{d}z} \qquad (7a)\\ \varepsilon_{zs} &= \frac{1}{2}\left\{\frac{\partial \tilde{u}_z}{\partial s} + \frac{\partial \tilde{u}_s}{\partial z}\right\}\\ &\approx \frac{1}{2}\left\{\frac{\mathrm{d}\psi_z^{U}(s)}{\mathrm{d}s}U(z) + \psi_s^{\theta}(s)\frac{\mathrm{d}\theta(z)}{\mathrm{d}z} + \psi_s^{\chi}(s)\frac{\mathrm{d}\chi(z)}{\mathrm{d}z}\right\} \qquad (7b)\\ \varepsilon_{ss} &= \frac{\partial \tilde{u}_s}{\partial s}\\ &= n\frac{\partial^2 u_n}{\partial s^2} = n\frac{\mathrm{d}^2\psi_n^{\chi}}{\mathrm{d}s^2}\chi(z) \qquad (7c)\end{aligned}$$

In obtaining equation (7c), the assumption of in-extensional contour is used. The strain component ε_{ss} in equation (7c) represents the bending deformation in the n–s plane, resulting from distortion of the contour. Unlike in thin-walled open beams where ε_{ss} is negligible, care must be taken not to ignore this component for the analysis of thin-walled closed beams.

Once the strain components are defined, the corresponding stresses can be easily found from the following constitutive relation:

$$\begin{aligned}\sigma_{zz} &= E_1(\varepsilon_{zz} + v\varepsilon_{ss})\\ \sigma_{ss} &= E_1(\varepsilon_{ss} + v\varepsilon_{zz})\\ \sigma_{sz} &= 2G\varepsilon_{sz}\end{aligned} \tag{8}$$

with

$$E_1 \equiv \frac{E}{1-v^2}$$

where E, G are Young's and shear moduli, respectively and v is Poisson's ratio.

For static analysis, the equilibrium equations can be obtained from the principle of the minimum potential energy [27] where the potential energy Π is expressed as

$$\Pi = \frac{1}{2}\int \sigma_{ij}\varepsilon_{ij}\,\mathrm{d}V - \int (p\tilde{u}_z + q\tilde{u}_s)\,\mathrm{d}V \tag{9}$$

where p and q are the external loads in the axial and tangential directions. Substituting equations (6)–(8) into equation (9) and integrating over the beam cross-section A yields

$$\begin{aligned}\Pi = \frac{1}{2}\int \{&aE_1U'^2 + cE_1\chi^2 + b_1G(U^2 + \theta'^2 + \chi'^2)\\ &+2G(b_1U\chi' + b_2U\theta' + b_2\theta'\chi')\}\mathrm{d}z\\ &-\int (p_1U + q_1\theta + q_2\chi)\mathrm{d}z\end{aligned} \tag{10}$$

where $(\ )'$ denotes the differentiation with respect to z. In equation (10), a, b_1, b_2 and c are defined as

$$\begin{aligned}a &= \int_A (\psi_z^U)^2\,\mathrm{d}A = \frac{b^2h^2(b+h)t}{24}\\ b_1 &= \int_A (\psi_s^\theta)^2\,\mathrm{d}A\\ &= \int_A (\psi_s^\chi)^2\,\mathrm{d}A\\ &= \int_A \left(\frac{\mathrm{d}\psi_z^U}{\mathrm{d}s}\right)^2\mathrm{d}A\\ &= \int_A \psi_s^\chi \frac{\mathrm{d}\psi_z^U}{\mathrm{d}s}\mathrm{d}A\\ &= \frac{bh(b+h)t}{2}\\ b_2 &= \int_A \psi_s^\theta \frac{\mathrm{d}\psi_z^U}{\mathrm{d}s}\,\mathrm{d}A\\ &= \int_A \psi_s^\theta\psi_s^\chi\,\mathrm{d}A = \frac{bh(b-h)t}{2}\end{aligned}$$

and

$$c = \int_A n^2 \left(\frac{\mathrm{d}^2 \psi_n^{\chi}}{\mathrm{d}s^2} \right)^2 \mathrm{d}A = \frac{8t^3}{b+h}$$

The one-dimensional load terms p_1, q_1 and q_2 are defined as

$$p_1 = \int_A p\psi_z^U \, \mathrm{d}A, \quad q_1 = \int_A q\psi_s^{\theta} \, \mathrm{d}A, \quad q_2 = \int_A q\psi_s^{\chi} \, \mathrm{d}A$$

The equilibrium equations and boundary conditions can be obtained from the following virtual work expression which may be found from the first variation of Π:

$$\begin{aligned} \int \{ & (-aE_1U'' + b_1GU + b_2G\theta' + b_1G\chi' - p_1)\delta U \\ & + (-b_2GU' - b_1G\theta'' - b_2G\chi'' - q_1)\delta\theta \\ & + (-b_1GU' - b_2G\theta'' - b_1G\chi'' + cE_1\chi - q_2)\delta\chi \} \, \mathrm{d}z \\ & + E_1(aU')\delta U|_{z_1}^{z_2} + G\{b_1\theta' + b_2(U+\chi')\}\delta\theta|_{z_1}^{z_2} \\ & + G\{b_1(\chi' + U) + b_2\theta'\}\delta\chi|_{z_1}^{z_2} = 0 \end{aligned} \tag{11}$$

where z_1 and z_2 are the axial co-ordinates denoting the beam ends.

The boundary terms in equation (11) represent the virtual work due to the external loads, and thus the following generalized stress resultants can be identified:

$$\begin{aligned} H &\equiv \int_A \sigma_{zs}\psi_s^{\theta} \, \mathrm{d}A \\ &= G(b_1\theta' + b_2U + b_2\chi') \end{aligned} \tag{12a}$$

$$\begin{aligned} B &\equiv \int_A \sigma_{zz}\psi_z^U \, \mathrm{d}A \\ &= E_1aU' \end{aligned} \tag{12b}$$

$$\begin{aligned} Q &\equiv \int_A \sigma_{zs}\psi_s^{\chi} \, \mathrm{d}A \\ &= G(b_1\chi' + b_1U + b_2\theta') \end{aligned} \tag{12c}$$

In equation (12), H is the usual twisting moment and B and Q are called the bimoment and the transverse bimoment, respectively.

FINITE ELEMENT FORMULATION

A standard two-noded displacement-based C^0 continuous thin-walled box beam element will be developed in this section. More elaborate approaches will definitely improve the solution convergence, but we do not pursue any of these as this paper is mainly concerned with showing a possibility of developing a new thin-walled closed beam element suitable for both static and dynamic analyses.

Using the linear field approximation typical in two-noded elements, the displacement vector $\mathbf{U}(z)$ is written as

$$\mathbf{U}(z) = \begin{Bmatrix} \theta(z) \\ U(z) \\ \chi(z) \end{Bmatrix} = \mathbf{N}\mathbf{d} \tag{13}$$

where the linear shape function matrix $\mathbf{N}$, and the nodal displacement vector $\mathbf{d}$ are given by

$$\mathbf{N} = \begin{bmatrix} \frac{1}{2}(1-\xi) & 0 & 0 & \frac{1}{2}(1+\xi) & 0 & 0 \\ 0 & \frac{1}{2}(1-\xi) & 0 & 0 & \frac{1}{2}(1+\xi) & 0 \\ 0 & 0 & \frac{1}{2}(1-\xi) & 0 & 0 & \frac{1}{2}(1+\xi) \end{bmatrix} \tag{14}$$

and

$$\mathbf{d} = \begin{Bmatrix} \theta_1 \\ U_1 \\ \chi_1 \\ \theta_2 \\ U_2 \\ \chi_2 \end{Bmatrix} \tag{15}$$

The dimensionless co-ordinate ξ used in equation (14) varies from -1 to 1 in an element.

The three dimensional displacement field $\tilde{\mathbf{u}}(n,s,z)$ can be written as

$$\tilde{\mathbf{u}}(n,s,z) = \begin{Bmatrix} \tilde{u}_z(n,s,z) \\ \tilde{u}_s(n,s,z) \\ \tilde{u}_n(n,s,z) \end{Bmatrix} = \mathbf{\Psi}(n,s)\mathbf{U}(z) \tag{16}$$

and equation (6) is used to write $\mathbf{\Psi}$ explicitly as

$$\mathbf{\Psi} = \begin{bmatrix} 0 & \psi_z^U & 0 \\ \psi_s^\theta & 0 & \psi_s^\chi + n\dfrac{\mathrm{d}\psi_n^\chi}{\mathrm{d}s} \\ \psi_n^\theta & 0 & \psi_n^\chi \end{bmatrix} \tag{17}$$

Using equation (7), the non-vanishing three-dimensional strains $\boldsymbol{\varepsilon}$ are given by

$$\boldsymbol{\varepsilon} = \begin{Bmatrix} \varepsilon_{zz} \\ 2\varepsilon_{zs} \\ \varepsilon_{ss} \end{Bmatrix} = \mathbf{L}\mathbf{N}\mathbf{d} = \mathbf{B}\mathbf{d} \tag{18}$$

where the linear operator $\mathbf{L}$ is defined as

$$\mathbf{L} = \begin{bmatrix} 0 & \psi_z^U \dfrac{\mathrm{d}}{\mathrm{d}z} & 0 \\ \psi_s^\theta \dfrac{\mathrm{d}}{\mathrm{d}z} & \dfrac{\mathrm{d}\psi_z^U}{\mathrm{d}s} & \psi_s^\chi \dfrac{\mathrm{d}}{\mathrm{d}z} \\ 0 & 0 & n\dfrac{\mathrm{d}^2\psi_n^\chi}{\mathrm{d}s^2} \end{bmatrix} \tag{19}$$

The substitution of equations (19) and (7) into equation (9) yields an approximate form of the potential energy Π

$$\Pi = \tfrac{1}{2}\mathbf{d}^{\mathrm{T}}\mathbf{K}\mathbf{d} - \mathbf{d}^{\mathrm{T}}\mathbf{P} - \mathbf{d}^{\mathrm{T}}\mathbf{Q} \tag{20}$$

where the potential energy from the generalized forces $\mathbf{Q}$ acting at nodes is also included. The element stiffness matrix $\mathbf{K}$ in equation (20) can be shown to be

$$\mathbf{K} = \int_{-1}^{1}\int_{A} \mathbf{B}^{\mathrm{T}}\mathbf{E}\mathbf{B}|J|\,\mathrm{d}A\,\mathrm{d}\xi \tag{21}$$

with the definition of the matrix $\mathbf{E}$

$$\mathbf{E} = \begin{bmatrix} E_1 & 0 & 0 \\ 0 & G & 0 \\ 0 & 0 & E_1 \end{bmatrix}$$

and the Jacobian J is simply the half of the element length l:

$$J = \frac{l}{2}$$

The generalized nodal load vector $\mathbf{Q}$ is defined as

$$\mathbf{Q} = \begin{Bmatrix} H_1 \\ B_1 \\ Q_1 \\ H_2 \\ B_2 \\ Q_2 \end{Bmatrix}$$

The generalized distributed load vector $\mathbf{P}$ is defined as

$$\begin{aligned} \mathbf{P} &= \int_{-1}^{1}\int_{A} \mathbf{N}^{\mathrm{T}}\,\tilde{\mathbf{R}}|J|\,\mathrm{d}A\,\mathrm{d}\xi \\ &= \int_{-1}^{1} \mathbf{N}^{\mathrm{T}}\mathbf{R}|J|\mathrm{d}\xi \end{aligned} \tag{22}$$

where $\tilde{\mathbf{R}}$ and $\mathbf{R}$ are defined as

$$\tilde{\mathbf{R}} = \begin{Bmatrix} q\psi_s^{\theta}(s) \\ p\psi_z^{U}(s) \\ q\psi_s^{\chi}(s) \end{Bmatrix}, \quad \mathbf{R} = \begin{Bmatrix} q_1 \\ p_1 \\ q_2 \end{Bmatrix}$$

Now invoking the stationarity of Π with respect to $\mathbf{d}$ yields the system of linear equations:

$$\frac{\partial \Pi}{\partial \mathbf{d}} = \mathbf{K}\mathbf{d} - (\mathbf{P} + \mathbf{Q}) = 0 \tag{23}$$

The explicit components of the stiffness matrix **K** can be obtained by either numerical or exact integration:

$$\mathbf{K}=\begin{bmatrix} G\frac{b_1}{l} & -G\frac{b_2}{2} & G\frac{b_2}{l} & -G\frac{b_1}{l} & -G\frac{b_2}{2} & -G\frac{b_2}{l} \\ & E_1\frac{a}{l}+G\frac{b_1 l}{3} & -G\frac{b_1}{2} & G\frac{b_2}{2} & -E_1\frac{a}{l}+G\frac{b_1 l}{6} & G\frac{b_1}{2} \\ & & G\frac{b_1}{l}+E_1\frac{cl}{3} & -G\frac{b_2}{l} & -G\frac{b_1}{2} & -G\frac{b_1}{l}+E_1\frac{cl}{6} \\ & & & G\frac{b_1}{l} & G\frac{b_2}{2} & G\frac{b_2}{l} \\ & -\text{sym}- & & & E_1\frac{a}{l}+G\frac{b_1 l}{3} & G\frac{b_1}{2} \\ & & & & & G\frac{b_1}{l}+E_1\frac{cl}{3} \end{bmatrix} \tag{24}$$

In order to derive the dynamic equations of motion, Hamilton's principle [27] can be used. Using the field approximation used for the derivation of the stiffness matrix, it is not difficult to obtain the following equations of motion:

$$\mathbf{M}\frac{\mathrm{d}^2\mathbf{d}}{\mathrm{d}t^2}+\mathbf{K}\mathbf{d}=\mathbf{P}+\mathbf{Q} \tag{25}$$

where $\mathbf{d}, \mathbf{P}$ and $\mathbf{Q}$ in equation (25) should now be treated as functions of time t, and the consistent mass matrix **M** is given by

$$\mathbf{M}=\int_{-1}^{+1}\int_A \mathbf{N}^{\mathrm{T}}\mathbf{\Psi}^{\mathrm{T}}\rho\mathbf{\Psi}\mathbf{N}|J|\,\mathrm{d}A\,\mathrm{d}\xi \tag{26}$$

where ρ is the density of the beam. In integrating equation (26) over the cross-section A, we propose to use $\psi_n^{\chi^*}$ instead of ψ_n^{χ}.

Neglecting terms equal to and higher than $O(t^2/bh)$, one may obtain the following expression for the element mass matrix **M**:

$$\mathbf{M}=\rho\begin{bmatrix} (b_1+d_1)\frac{l}{3} & 0 & (b_2+d_3)\frac{l}{3} & (b_1+d_1)\frac{l}{6} & 0 & (b_2+d_3)\frac{l}{6} \\ & a\frac{l}{3} & 0 & 0 & a\frac{l}{6} & 0 \\ & & (b_1+d_2)\frac{l}{3} & (b_2+d_3)\frac{l}{6} & 0 & (b_1+d_2)\frac{l}{6} \\ & & & (b_1+d_1)\frac{l}{3} & 0 & (b_2+d_3)\frac{l}{3} \\ & -\text{sym} & & & a\frac{l}{3} & 0 \\ & & & & & (b_1+d_2)\frac{l}{3} \end{bmatrix} \tag{27}$$

where ρ is the mass density and the additional constants d_1, d_2 and d_3 are defined as

$$d_1 = \frac{(b^3 + h^3)t}{6}$$
$$d_2 = \frac{17(b^3 + h^3)t}{70}$$
$$d_3 = \frac{(b^3 - h^3)t}{5}$$

For free-vibration analysis, the load terms **P** and **Q** will be dropped.

NUMERICAL RESULTS

Example 1 (*Box beam under prescribed warping displacement*). Figure 2 shows a thin-walled box beam ($L = 500\,\text{mm}$, $b = 25\,\text{mm}$, $h = 50\,\text{mm}$, $t = 1\,\text{mm}$, $E = 200\,\text{GN/m}^2$, $G = 76{\cdot}9\,\text{GN/m}^2$) with one-end fixed and the other-end free. When a unit warping displacement U ($U/t = 1$) is prescribed at the free end, this problem cannot be solved by the Timoshenko or Euler beam elements. Therefore, either plate elements or thin-walled closed beam elements like the present one must be employed. The displacements (u_z, u_x) in the z and x directions at $x = 12{\cdot}5\,\text{mm}$, $y = 25\,\text{mm}$ are obtained as a function of z in Figure 3. The displacements in Figure 3(a) and 3(b) actually represent the warping and distortional displacements, respectively. The converging results from the present thin-walled box beam element agree well with those obtained from the NASTRAN [28] plate element (element type: QUAD4). The converging result is obtained with the 15 present elements.[§]

To examine the convergence behavior of the present element, the displacement in the x direction at $x = 12{\cdot}5\,\text{mm}$, $y = 25\,\text{mm}$, $z = 500\,\text{mm}$ is obtained with an increasing number of the present elements. The numerical results are plotted in Figure 4. Although the present results converge, the convergence rate is not rapid. This slow convergence is attributed to the fact that the displacements actually vary exponentially [2]. This observation suggests the development of more rapidly converging elements, but this will not be pursued any further in the present work.

Example 2 (*Box beam subjected to a twisting moment*). A problem that can be handled by the usual Euler or Timoshenko beam elements is considered. The box beam is loaded by a twisting moment of magnitude $H = 100\,\text{N m}$ at one end whose cross section is rigidly constrained. Table I shows the magnitude of the tip rotation.

The conventional beam result is also satisfactory, but this problem is only considered to show that the present element gives an accurate result in this limiting case. Note that even in this case, there exists warping deformation, although small, which cannot be predicted by the conventional beam elements: see Figure 5 for the interior warping displacement obtained from the axial displacement along the z-axis ($x = 12{\cdot}5\,\text{mm}$, $y = 25\,\text{mm}$). The result is normalized with respect to the maximum warping displacement at $x = 250\,\text{mm}$ calculated by the NASTRAN plate elements. Again, an excellent agreement between the results from the present thin-walled box beam and plate elements is observed.

[§]The total number of the QUAD4 elements is as many as 2600. However, a smaller number of plate elements may be sufficient in obtaining the converging results, but the NASTRAN results are obtained only to be compared with the present results

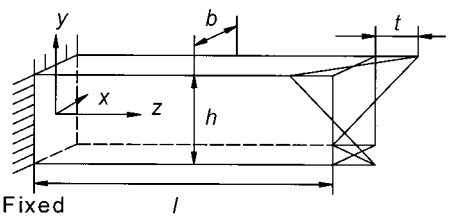

Figure 2. A cantilevered thin-walled box beam under the prescribed unit warping displacement

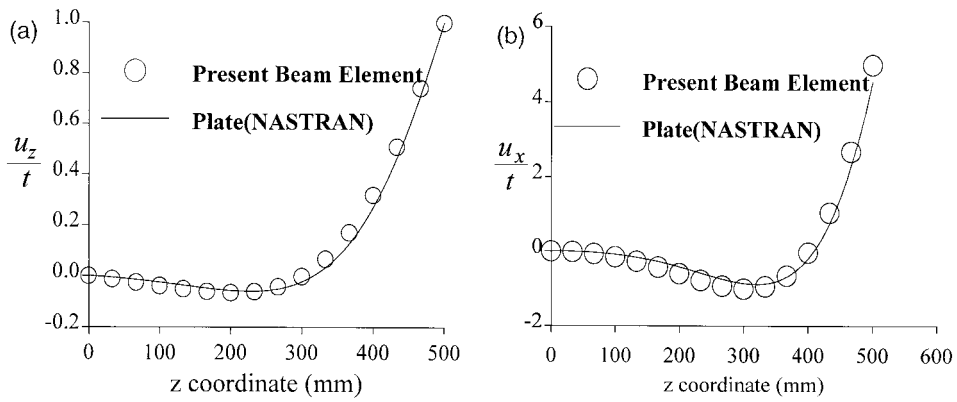

Figure 3. The displacements: (a) in the z direction; and (b) in the x direction at $x = 12{\cdot}5$ mm, $y = 25$ mm of a box beam under the unit warping displacement

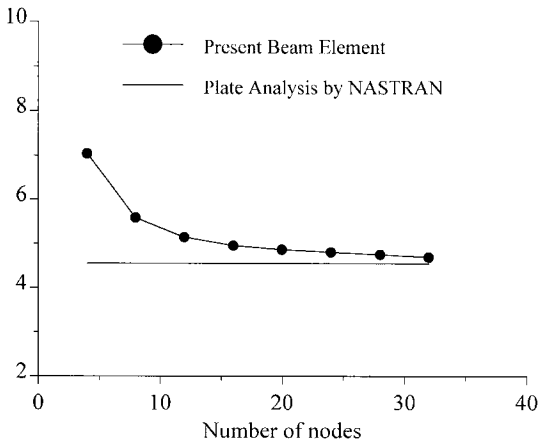

Figure 4. The convergence of the displacement in the x direction at $x = 12{\cdot}5$ mm, $y = 25$ mm, $z = 500$ mm for the beam shown in Figure 2. The results by the present box beam elements are compared with the results by the NASTRAN plate elements

Table I. The tip rotation at the loaded end of a box beam under a tip twisting moment

Plate	Conventional beam	Present ($N_e = 2$)	Present ($N_e = 8$)	Present ($N_e = 15$)
$1{\cdot}554 \times 10^{-2}$	$1{\cdot}560 \times 10^{-2}$	$1{\cdot}511 \times 10^{-2}$	$1{\cdot}554 \times 10^{-2}$	$1{\cdot}556 \times 10^{-2}$

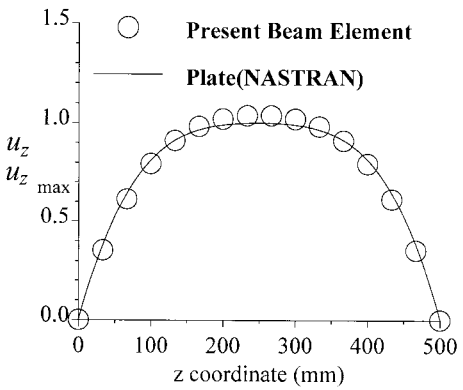

Figure 5. The axial displacement at $x = 12{\cdot}5$ mm, $y = 25$ mm of a box beam subjected to a twisting moment. The symbol $u_z|_{\max}$ is the maximum displacement at $z = 250$ mm calculated from the NASTRAN plate elements

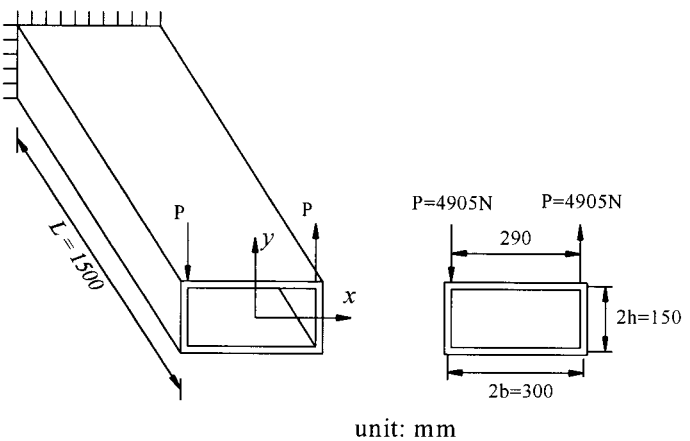

Figure 6. A built-in box beam in one end which is subjected to a couple

Example 3 (*Box beam subjected to a couple*). A cantilevered box beam ($E = 196{\cdot}2\,\text{kN/mm}^2$ and $v = 0{\cdot}27$, $t = 3{\cdot}18$ mm) subjected to a couple at the end, which was studied by Paavola [14] and Boswell and Zhang [6], is solved by the present element. Balch [24] also solved this problem using a perturbation technique. The applied couple causes distortion as well as torsion as indicated by Figure 6. In Figure 7(a), the present result for the angle of rotation θ, plotted as the function of the axial co-ordinate z, is compared with the existing results. Figure 7(b) shows the distribution

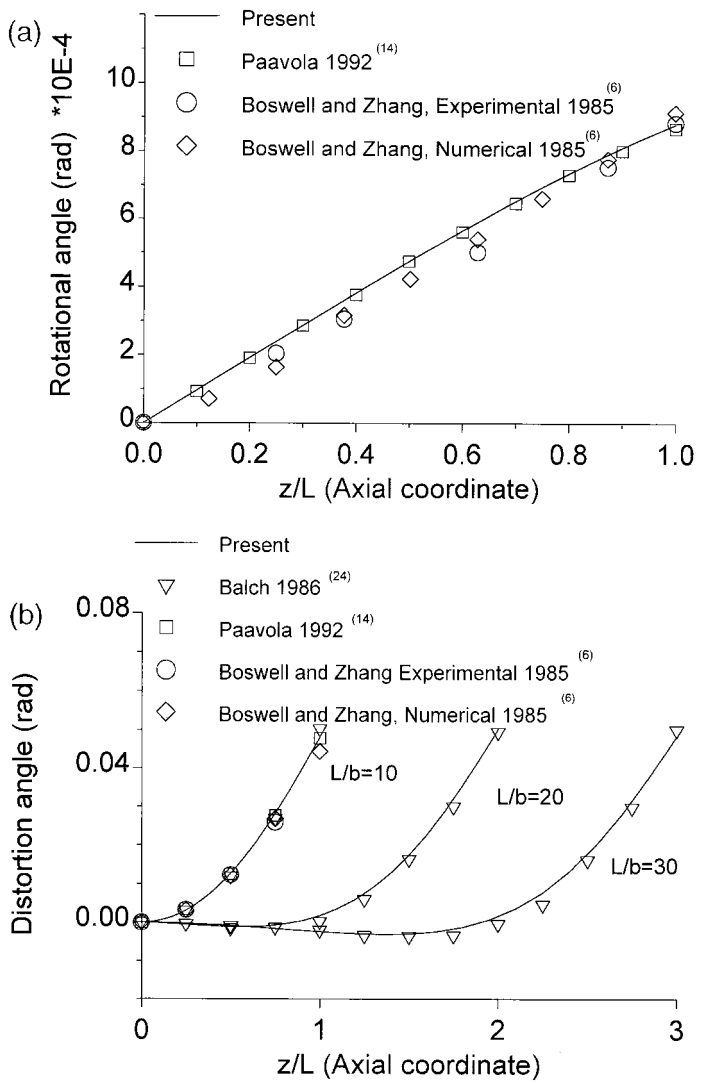

Figure 7. (a) The angle of the axial rotation θ; and (b) the angle of the distortion χ as functions of z for the box beam in Figure 6

of the angle of distorsion χ for various beam lengths. The good agreement of the present result with others is observed.

Example 4 (*Free vibration analysis of a rectangular box beam with both ends free*). Now we consider the free vibration of steel rectangular box beams ($h = 50\,\text{mm}$, $L = 500\,\text{mm}$, $t = 1\,\text{mm}$) with varying values of h/b. Although vibration problems are as important as static problems, no report on finite element vibration analysis that takes the distortional effects into account has been reported and, therefore, a comparison with other results cannot be made.

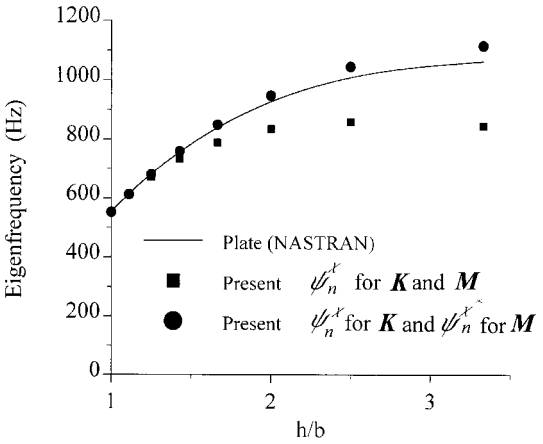

Figure 8. The variation of the first eigenfrequencies for varying ratios of h/b. Squares denote the present results with the use of ψ_n^{χ} for both stiffness and mass matrices. Circles denote the results with the use of ψ_n^{χ} and $\psi_n^{\chi^*}$ for the construction of the stiffness and mass matrices, respectively

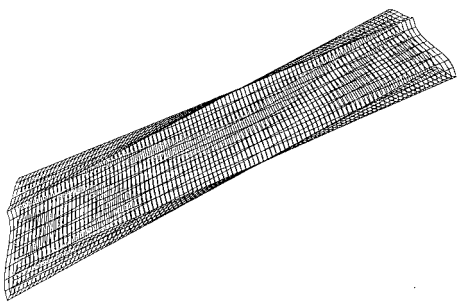

Figure 9. Torsional mode coupled with distortion and warping deformations in a rectangular box beam with a free-free end condition (obtained from the NASTRAN plate elements)

Figure 8 shows the first eigenfrequencies for varying values of h/b. The results obtained by the present box beam elements are compared with the NASTRAN plate element results. The corresponding mode obtained from the NASTRAN plate elements is also shown in Figure 9 for reference. In Figure 8, the results marked by squares are those obtained when the same ψ_n^{χ} is used for the construction of both **M** and **K**. To obtain the results marked by circles, ψ_n^{χ} and $\psi_n^{\chi^*}$ are used for the construction of **M** and **K**, respectively. The results in Figure 8 clearly indicate that the present formulation based on the statically admissible stiffness and kinematically compatible mass matrices gives good results for the wide range of h/b.

It is interesting to note that for $h/b = 1$, the first mode is distortional and a rotational dominated mode appears as a higher mode. This behaviour is quite different from those of thin-walled open beams. Such distortional modes are known to affect quite significantly the dynamic behaviour near the joints of thin-walled box beams [26], and these modes are well predicted in the present finite element analysis.

Table II. The first eigenfrequencies of a rectangular box beam with a fixed-free end condition

Mode number	Plate	Conventional beam	Present ($N_e = 15$)
1st mode	852·64 Hz	—	873·74 Hz

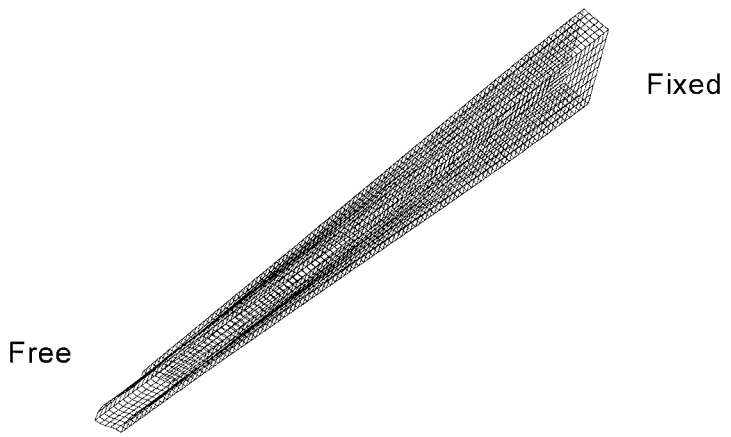

Figure 10. Torsional mode coupled with distortion and warping deformations in a rectangular box beam with a fixed-free end condition (obtained from the NASTRAN plate elements)

Table III. The eigenfrequencies of a square box beam with a fixed-free end condition

Mode	Plate	Conventional beam	Present ($N_e = 15$)
Distortion	569·68 Hz	—	573·78 Hz
Tortion	1342·23 Hz	1359·6 Hz	1360·2 Hz

Example 5 (*Vibration analysis of a rectangular box beam with a fixed-free end condition*). We also carry out the vibration anlaysis of a rectangular box beam with one end fixed and the other end free ($b = 25$ mm, $h = 50$ mm, $L = 500$ mm, $t = 1$ mm). Table II lists the first eigenfrequency, and Figure 10 shows the first vibration mode. The conventional beam theory is not useful to predict the first eigenfrequency. The present result shows a good agreement with the plate element result.

Example 6 (*Vibration analysis of a square box beam with a fixed-free end condition*). In the case of a square box beam ($b = h = 50$ mm, $L = 500$ mm, $t = 1$ mm) torsional and distortional deformations are uncoupled. The lowest distortional and torsional eigenfrequencies are tabulated in Table III, which are compared with other results.

CONCLUSIONS

A new C^0-continuous displacement-based box beam finite element has been proposed in the present study. Direct kinematic variables representing torsion, warping and distortion were used so that the present formulation was shown to be suitable for both static and dynamic analyses. The present use of statically admissible and kinematically compatible in-plane distortional functions for stiffness and mass matrices was shown to give satisfactory results for a wide range of beam width-to-height ratios. Several numerical examples have confirmed that the present elements accurately predict the dynamic behaviour of the coupled deformations of torsion, warping, and distortion. Work is in progress to develop more general thin-walled beam elements, which is based on the present analysis.

REFERENCES

1. Timoshenko SP, Gere JM. *Theory of Elastic Stability*; 2nd ed. McGraw-Hill: New York, 1961.
2. Vlasov VZ. *Thin Walled Elastic Beams*; Israel Program for Scientific Translations, Jerusalem, 1961.
3. Křistek, V. Tapered box girders of deformable cross section. *Journal of the Structural Division ASCE* 1970; **96**(ST8):1761–1793. Proc. Paper 7489.
4. Boswell LF, Zhang SH. A box beam finite element for the elastic analysis of thin-walled structures. *Thin-Walled Structures* 1983;**1**:353–383.
5. Boswell LF, Zhang SH. The effect of distortion in thin-walled box-spine beams. *International Journal of Solids and Structures* 1984;**20**(9/10):845–862.
6. Boswell LF, Zhang SH. An experimental investigation of the behavior of thin-walled box beams. *Thin-Walled Structures* 1985;**3**:35–65.
7. Zhang SH, Lyons LPR. A thin-walled box beam finite element for curved bridge analysis. *Computers and Structures* 1984;**18**(6):1035–1046.
8. Zhang SH, Lyons LPR. The application of the thin-walled box beam element to multibox bridge analysis. *Computers and Structures* 1984;**18**(5):795–802.
9. Boswell LF, Li Q. Consideration of the relationships between torsion, distortion and warping of thin-walled beams. *Thin-Walled Structures* 1995;**21**:147–161.
10. Razaqpur AG, Li HG. Thin-walled multicell box girder finite element. *Journal of Structural Engineering* ASCE 1991;**117**(10):2953–2971.
11. Razaqpur AG, Li HG. A finite element with exact shape functions for shear lag analysis in multi-cell box-girders. *Computers and Structures* 1991;**39**(1/2):155–163.
12. Razaqpur AG, Li HG. Refined analysis of curved thin-walled multicell box girders. *Computers and Structures* 1994;**53**(1):131–142.
13. Mikkola MJ, Paavola J. Finite element analysis of box girders. *Journal of the Structural Division ASCE* 1980;**106**:1343–1357.
14. Paavola J. A finite element technique for thin-walled girders. *Computers and Structures* 1992;**44**:159–175.
15. Prokic A. Thin-walled beams with open and closed cross-sections. *Computers and Structures* 1993;**47**(6):1065–1070.
16. Gere JM. Torsional vibrations of beams of thin-walled open section. *Journal of Applied Mechanics* 1954;**21**:381–387.
17. Bishop RED, Price WG, Cheng ZX. On the structural dynamics of a Vlasov beam. *Proceedings of the Royal Society of London A* 1983;**388**:49–73.
18. Friberg PO. Beam element matrices derived from Vlasov's theory of open thin-walled elastic beams. *International Journal for Numerical Methods in Engineering* 1985;**21**:1205–1228.
19. Zhang Z, Chen S. Dynamic finite-element method of thin-walled beams. *AIAA Journal* 1990;**28**(5):910–914.
20. Kou CH, Benzley SE, Huang JY, Firmage DA. Free vibration analysis of curved thin-walled girder bridges. *Journal of Structural Engineering* 1992;**118**(10):2890–2910.
21. Kim MY, Chang SP, Kim SB. Spatial stability and free vibration of shear flexible thin-walled elastic beams. I: Analytical approach. *International Journal for Numerical Methods in Engineering* 1994;**37**:4097–4115.
22. Kim MY, Chang SP, Kim SB. Spatial stability and free vibration of shear flexible thin-walled elastic beams. II: Numerical approach. *International Journal for Numerical Methods in Engineering* 1994;**37**:4117–4140.
23. Laudiero F, Savoia M. The shear strain influence on the dynamics of thin-walled beams. *Thin-Walled Structures* 1991;**11**:375–407.

24. Balch CD. End effects in thin-walled box beams and tubular frame joints. *Ph.D. Dissertation*, Stanford University, Stanford, CA, 1986.
25. Balch CD, Steele CR. Asymptotic solutions for warping and distortion of thin-walled box beams. *Journal of Applied Mechanics* 1987;**54**:165–173.
26. Kim YY, Yim HJ, Kang JH, Kim JH. Reconsideration of the joint modelling technique: in a box-beam T-joint. SAE 951108, 1995:275–279.
27. Washizu K. *Variational Methods in Elasticity and Plasticity*; 3rd ed. Pergamon Press: London, 1982.
28. MSC/NASTRAN. *User's Manual*; The Macneal Swendler Corporation: Los Angeles, 1989.

